High-performance InGaN-based green light-emitting diodes with quaternary InAlGaN/GaN superlattice electron blocking layer

An-Jye Tzou,[1,2] Da-Wei Lin,[2] Chien-Rong Yu,[2] Zhen-Yu Li,[3] Yu-Kuang Liao,[2] Bing-Cheng Lin,[2] Jhih-Kai Huang,[2] Chien-Chung Lin,[3] Tsung Sheng Kao,[2] Hao-Chung Kuo,[1,*] and Chun-Yen Chang[1,4]

[1]*Department of Electrophysics, National Chiao Tung University, Hsinchu 30010, Taiwan*
[2]*Department of Photonics and Institute of Electro-Optical Engineering, National Chiao Tung University, Hsinchu 30010, Taiwan*
[3]*Epistar, 22 Keya Road, Daya, Central Taiwan Science Park, Taichung 42881, Taiwan*
[4]*Research Center for Applied Sciences, Academia Sinica, 128 Academia Road, Section 2, Nankang, Taipei 11529, Taiwan*
[*]*hckuo@faculty.nctu.edu.tw*

Abstract: In this study, high-performance InGaN-based green light-emitting diodes (LEDs) with a quaternary InAlGaN/GaN superlattice electron blocking layer (QSL-EBL) have been demonstrated. The band structural simulation was employed to investigate the electrostatic field and carriers distribution, show that the efficiency and droop behavior can be intensively improved by using a QSL-EBL in LEDs. The QSL-EBL structure can reduce the polarization-related electrostatic fields in the multiple quantum wells (MQWs), leading to a smoother band diagram and a more uniform carriers distribution among the quantum wells under forward bias. In comparison with green LEDs with conventional bulk-EBL structure, the light output power of LEDs with QSL-EBL was greatly enhanced by 53%. The efficiency droop shows only 30% at 100 A/cm^2 comparing to its peak value, suggesting that the QSL-EBL LED is promising for future white lighting with high performance.

OCIS codes: (230.3670) Light-emitting diodes; (230.2090) Electro-optical devices.

References and links

1. S. Mutu, F. J. P. Schuurmans, and M. D. Pashley, "Red, green and blue LEDs for white light illumination," IEEE J. Sel. Top. Quantum Electron. **8**(2), 333–338 (2002).
2. E. Fred Schubert, *Light-Emitting Diodes* (Cambridge, 2006).
3. F. Bernardini, V. Fiorentini, and D. Vanderbilt, "Spontaneous polarization and piezoelectric constants of III-V nitrides," Phys. Rev. B **56**(16), R10024 (1997).
4. Z. H. Zhang, S. T. Tan, Z. Ju, W. Liu, Y. Ji, Z. Kyaw, Y. Dikme, X. W. Sun, and H. V. Demir, "On the effect of step-doped quantum barriers in InGaN/GaN light emitting diodes," J. Disp. Technol. **9**(4), 226–233 (2013).
5. Z. H. Zhang, W. Liu, Z. Ju, S. T. Tan, Y. Ji, Z. Kyaw, X. Zhang, L. Wang, X. W. Sun, and H. V. Demir, "Self-screening of the quantum confined Stark effect by the polarization induced bulk charges in the quantum barriers," Appl. Phys. Lett. **104**(24), 243501 (2014).
6. R. M. Farrell, P. S. Hsu, D. A. Haeger, K. Fujito, S. P. DenBaars, J. S. Speck, and S. Nakamura, "Low-threshold-current-density AlGaN-cladding-free m-plane InGaN/GaN laser diodes," Appl. Phys. Lett. **96**(23), 231113 (2010).
7. M. R. Krames, O. B. Shchekin, R. Mueller-Mach, G. O. Mueller, L. Zhou, G. Harbers, and M. George Craford, "Status and future of high-power light-emitting diodes for solid-state lighting," J. Disp. Technol. **3**(2), 160–175 (2007).
8. K. J. Vampola, M. Iza, S. Keller, S. P. DenBaars, and S. Nakamura, "Measurement of electron overflow in 450 nm InGaN light-emitting diode structures," Appl. Phys. Lett. **94**(6), 061116 (2009).
9. M. F. Schubert, J. Xu, J. K. Kim, E. F. Schubert, M. H. Kim, S. Yoon, S. M. Lee, C. Sone, T. Sakong, and Y. Park, "Polarization-matched GaInN/AlGaInN multi-quantum-well light-emitting diodes with reduced efficiency droop," Appl. Phys. Lett. **93**(4), 041102 (2008).
10. Y.-K. Kuo, J.-Y. Chang, M.-C. Tasi, and S.-H. Yen, "Advantages of blue InGaN multiple-quantum well light-emitting diodes with InGaN barriers," Appl. Phys. Lett. **95**(1), 011116 (2009).

#261098 Received 22 Mar 2016; revised 6 Apr 2016; accepted 9 Apr 2016; published 17 May 2016

11. Z. H. Zhang, W. Liu, Z. Ju, S. T. Tan, Y. Ji, X. Zhang, L. Wang, Z. Kyaw, X. W. Sun, and H. V. Demir, "Polarization self-screening in [0001] oriented InGaN/GaN light-emitting diodes for improving the electron injection efficiency," Appl. Phys. Lett. **104**(25), 251108 (2014).
12. C. H. Wang, C. C. Ke, C. Y. Lee, S. P. Chang, W. T. Chang, J. C. Li, Z. Y. Li, H. C. Yang, H. C. Kuo, T. C. Lu, and S. C. Wang, "Hole injection and efficiency droop improvement in InGaN/GaN light-emitting diodes by band-engineered electron blocking layer," Appl. Phys. Lett. **97**(26), 261103 (2010).
13. Z. H. Zhang, Z. Ju, W. Liu, S. T. Tan, Y. Ji, Z. Kyaw, X. Zhang, N. Hasanov, X. W. Sun, and H. V. Demir, "Improving hole injection efficiency by manipulating the hole transport mechanism through p-type electron blocking layer engineering," Opt. Lett. **39**(8), 2483–2486 (2014).
14. J. H. Park, D. Y. Kim, S. Hwang, D. Meyaard, E. F. Schubert, Y. D. Han, J. W. Choi, J. Cho, and J. K. Kim, "Enhanced overall efficiency of GaInN-based light-emitting diodes with reduced efficiency droop by Al-composition-graded AlGaN/GaN superlattice electron blocking layer," Appl. Phys. Lett. **103**(6), 061104 (2013).
15. Y.-K. Kuo, M.-C. Tasi, and S.-H. Yen, "Numerical simulation of blue InGaN light-emitting diodes with polarization-matched AlGaInN electron-blocking layer and barrier layer," Opt. Commun. **282**(21), 4252–4255 (2009).
16. J. Kang, H. Li, Z. Li, Z. Liu, P. Ma, X. Yi, and G. Wang, "Enhancing the performance of green GaN-based light-emitting diodes with graded superlattice AlGaN/GaN inserting layer," Appl. Phys. Lett. **103**(10), 102104 (2013).
17. B. C. Lin, K. J. Chen, H. V. Han, Y. P. Lan, C. H. Chiu, C. C. Lin, M. H. Shih, P.-T. Lee, and H.-C. Kuo, "Advantages of blue LEDs with graded-composition AlGaN/GaN superlattice EBL," IEEE Photonics Technol. Lett. **25**(21), 2062–2065 (2013).
18. Y. Y. Zhang and Y. A. Yin, "Performance enhancement of blue light-emitting diodes with a special designed AlGaN/GaN superlattice electron-blocking layer," Appl. Phys. Lett. **99**(22), 221103 (2011).
19. S. J. Lee, S. H. Han, C. Y. Cho, S. P. Lee, D. Y. Noh, H. W. Shim, Y. C. Kim, and S. J. Park, "Improvement of GaN-based light-emitting diodes using p-type AlGaN/GaN superlattices with a graded Al composition," J. Phys. D Appl. Phys. **44**(10), 105101 (2011).
20. C. S. Xia, Z. M. Simon Li, Z. Q. Li, and Y. Sheng, "Effect of multiquantum barriers in performance enhancement of GaN-based light-emitting diodes," Appl. Phys. Lett. **102**(1), 013507 (2013).
21. H. Hirayama, Y. Tsukada, T. Maeda, and N. Kamata, "Marked enhancement in the efficiency of deep-ultraviolet AlGaN light-emitting diodes by using a multiquantum-barrier electron blocking layer," Appl. Phys. Express **3**(3), 031002 (2010).
22. C. S. Chang, Y. K. Su, S. J. Chang, P. T. Chang, Y. R. Wu, K. H. Huang, and T. P. Chen, "High-brightness AlGaInP 573-nm light-emitting diode with a chirped multiquantum barrier," IEEE J. Quantum Electron. **34**(1), 77–83 (1998).
23. T. Takagi, F. Koyama, and K. Iga, "Design and photoluminescence study on a multiquantum barrier," IEEE J. Quantum Electron. **27**(6), 1511–1519 (1991).
24. Y. Y. Zhang, X. L. Zhu, Y. A. Yin, and J. Ma, "Performance enhancement of near-UV light-emitting diodes with an InAlN/GaN superlattice electron-blocking layer," IEEE Electron Device Lett. **33**(7), 994–996 (2012).
25. J. Lee, P. G. Eliseev, M. Osinski, D. S. Lee, D. I. Florescu, and M. Pophristic, "InGaN-based ultraviolet emitting heterostructures with quaternary AlInGaN barriers," IEEE J. Sel. Top. Quantum Electron. **9**(5), 1239–1245 (2003).
26. S. M. Thahab, H. Abu Hassan, and Z. Hassan, "InAlGaN quaternary multi-quantum wells UV laser Diode performance and characterization," World Acad. Sci. Eng. Technol. **55**, 352–355 (2009).
27. J. P. Zhang, E. Kuokstis, Q. Fareed, H. Wang, J. W. Yang, G. Simin, M. A. Khan, R. Gaska, and M. S. Shur, "Pulsed atomic layer epitaxy of quaternary AlInGaN layers," Appl. Phys. Lett. **79**(7), 925–927 (2001).
28. C. T. Yu, W. C. Lai, C. H. Yen, and S. J. Chang, "InN/GaN alternative growth of thick InGaN wells on GaN-based light emitting diodes," Opt. Mater. Express **3**(11), 1952–1959 (2013).
29. I. Vurgaftman and J. R. Meyer, "Band parameters for nitrogen-containing semiconductors," J. Appl. Phys. **94**(6), 3675–3696 (2003).

1. Introduction

In recent years, high efficiency light-emitting diodes (LEDs) have attracted intensive attentions due to their wide applications in solid-state lighting and functional display technology [1,2]. However, the InGaN-based green LED suffers a relatively lower internal quantum efficiency due to various reasons. First, the high In content required in active region (In~30%) brings many great challenges in strain management. Second, influences of strain-induced internal polarization field are also aggravated. Band diagrams of quantum wells (QWs) in green LED is more tilted than those of blue ones, and the electron and hole wave functions overlap becomes weaker [3–6], resulting in lower recombination rate and poor internal quantum efficiency (EQE). The drastic performance deterioration of LEDs in green spectral region is also known as "green gap" in the community [7]. The highly-tilted band diagram also leads to a serious "efficiency droop" in InGaN-based green LEDs, which has been attributed to the enhanced carrier overflow out of the active region and inefficient hole transport [8]. In general, $Al_xGa_{1-x}N$ electron blocking layer (EBL) was inserted in LED

#261098 Received 22 Mar 2016; revised 6 Apr 2016; accepted 9 Apr 2016; published 17 May 2016

structures to suppress electron leakage. However, the electron-blocking function becomes less effective due to the band bending caused by the large electrostatic field. The band bending not only reduces the barrier height for electron leakage but also increases the effective barrier height for hole injection, leading to a strong efficiency droop [9–11]. Several designs of EBL structure have been reported, for example, graded-composition EBL (GEBL) [12], AlGaN/GaN/AlGaN-type EBL [13], Al-composition-graded AlGaN/GaN superlattice EBL (GSL-EBL) [14], polarization-matched quaternary InAlGaN EBL [15], and ternary AlGaN/GaN superlattice EBL (SL-EBL) to mitigate the efficiency droop [16–24]. In this paper, we demonstrated a quaternary superlattice electron blocking layer (QSL-EBL) design for droop improvement in green LEDs. The quaternary InAlGaN alloy created a design space for EBL with polarization matching to GaN [25]. Hence the quaternary EBL can mitigate the bend bending between the last barrier and EBL due to suppressed piezoelectric field, leading to decrease barrier height for holes. In addition, the SL-EBL would also raise the effective barrier height for blocking electron overflow by means of the interference among electron wave function scattered by superlattice interfaces. Therefore, the QSL-EBL can significantly increase the potential barrier height for electrons and leads to lower effective barrier height for holes simultaneously.

However, the growth of quaternary InAlGaN by metal organic chemical vapor deposition (MOCVD) was regarded very challenging due to the significant differences among the optimal growth temperatures among AlN, InN, and GaN. A lower growth temperature favors In incorporation, but the diffusion length of Al adatoms will be further reduced [26]. Some of research groups investigated the deposition of InAlGaN-based MQWs by using pulsed atomic layer epitaxy (PALE) [27]. PALE technology successfully reduced the growth temperature below 800°C to deposit quaternary alloy. Additionally, Yu *et al.* also reported to grow high indium incorporated InGaN/GaN MQWs by using digital growth procedure [28]. Therefore, we propose to fabricate the QSL-EBL by digital growth procedure. Taking the growth quality into consideration, the performance improvements of designed LEDs were studied and investigated in this work.

2. Experiments and simulations

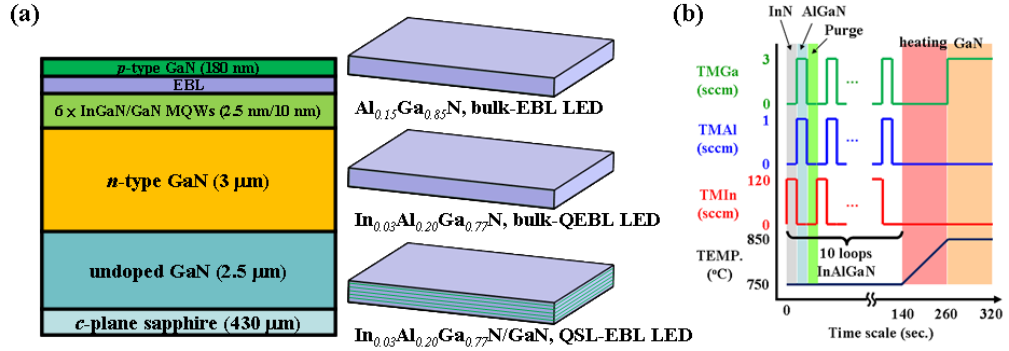

Fig. 1. Schematic diagram of the LED structure for bulk-EBL LED, bulk-QEBL LED, and QSL-EBL LED, respectively. (b) Growth procedure schematic diagram of the quaternary $In_{0.03}Al_{0.2}Ga_{0.77}N$/GaN superlattice EBL (QSL-EBL).

The epitaxial InGaN-based green LED structures were grown by a low-pressure MOCVD system with a vertical reactor chamber. The LED structures were grown on sapphire substrates, started from a sputtered AlN nucleation layer, a 2.5-μm-thick undoped GaN layer and a 3-μm-thick *n*-type GaN layer ($[N_D] = 5 \times 10^{18}$ cm^{-3}). The active region was consisted of six 2.5-nm-thick $In_{0.27}Ga_{0.85}N$ multiple-quantum wells (MQWs), sandwiched by seven 10-nm-thick GaN barrier layers. For conventional LED, a 20-nm-thick *p*-$Al_{0.15}Ga_{0.85}N$ bulk EBL ($[N_A] = 3 \times 10^{17}$ cm^{-3}) and a 180-nm-thick *p*-type GaN layer ($[N_A] = 5 \times 10^{17}$ cm^{-3}) were

#261098 Received 22 Mar 2016; revised 6 Apr 2016; accepted 9 Apr 2016; published 17 May 2016

grown on the top of active region (denoted as bulk-EBL LED). Another LED structure (denoted as QSL-EBL LED) kept similar structures except for the conventional *p*-AlGaN EBL, which was replaced by the *p*-$In_{0.03}Al_{0.20}Ga_{0.77}N$/GaN QSL-EBL ($[N_A] = 3 \times 10^{17}$ cm^{-3}). The QSL-EBL was consisted of five 2-nm-thick GaN wells, sandwiched by six 2-nm-thick $In_{0.03}Al_{0.20}Ga_{0.77}N$ barriers. In addition, we simulated a LED structure with bulk $In_{0.03}Al_{0.20}Ga_{0.77}N$ EBL (denoted as bulk-QEBL LED) for investigation and comparison. The thickness of bulk QEBL was 20-nm-thick *p*-$In_{0.03}Al_{0.20}Ga_{0.77}N$ ($[N_A] = 3 \times 10^{17}$ cm^{-3}). Figure 1(a) shows the schematic diagram of the sample structures for bulk-EBL LED, bulk-QEBL LED, and QSL-EBL LED, respectively. Furthermore, the quaternary InAlGaN barrier layer was prepared by the InN/AlGaN digital growth method. The growth temperature of the quaternary InAlGaN barrier layer was kept at 750°C. The pulse durations of InN and AlGaN for each InAlGaN layer were kept in 4 sec/ 4 sec with 10 loops. After one cycle of InN/AlGaN was deposited, a purged pulse with hydrogen was kept in 6 sec for enhancing migration of Al adatoms, as shown in Fig. 1(b). The flow rates and V/III ratios of digital growth are listed and shown in Table 1. Subsequently, the LED mesa with an area of 300 × 300 μm^2 was defined by photolithography and dry etching process. In addition, a transparent conduction indium-tin-oxide (ITO) layer was employed to be the current spreading layer and Ni/Au metal was deposited as *p*-type and *n*-type electrodes, respectively. The emission wavelengths of all LEDs were around 550 nm.

Table 1. The precursor flow rate, V/III ratio, and pulse duration of digital growth procedure for QSL-EBL.

	TMIn flow (μmole/min)	TMGa flow (μmole/min)	TMAl flow (μmole/min)	NH_3 flow (mole/min)	V/III Ratio	Pulse duration (sec.)
InN	28	-	-	0.4	14000	4
AlGaN	-	7.7	1.5	0.4	52000	4

Regarding the structural analysis of the superlattice layer, the transmission electron microscopy (TEM, model: JOEL ARM-200F) and the secondary ion mass spectroscopy (SIMS) were employed to identify the QSL-EBL structure. The full structure of QSL-EBL is illustrated in the high-angle annular dark field (HAADF) image from scanning transmission electron microscopy (STEM) as shown in Fig. 2(a). The thickness formation of QSL-EBL is identified by high resolution bright field TEM image, as shown in Fig. 2(b). The QSL-EBL structures with darker and brighter bands present the GaN wells and InAlGaN barriers respectively. In addition, an intensity line profile across the region of QSL-EBL was traced from Fig. 2(b) as the red line, which is corresponding to the Fig. 2(c). It should be noticed that the clearly interfaces between $In_{0.03}Al_{0.20}Ga_{0.77}N$ barriers and GaN wells in QSL-EBL are clearly observed. The intensity profile from the high resolution bright field image show that the thickness of the InAlGaN layers is kept as 2.067 nm. Also the sharp interfaces can be obviously identified from the line scan result. Following the SIMS spectra show that the content of QSL-EBL, as shown in Fig. 2(d). The concentrations of Ga, Al, and In atoms were defined as atomic fraction and the ~3% of In atomic fraction was obtained, along with ~20% of Al content. As a result, we successfully grown the InGaN-based green LED with QSL-EBL via digital growth method.

#261098 Received 22 Mar 2016; revised 6 Apr 2016; accepted 9 Apr 2016; published 17 May 2016

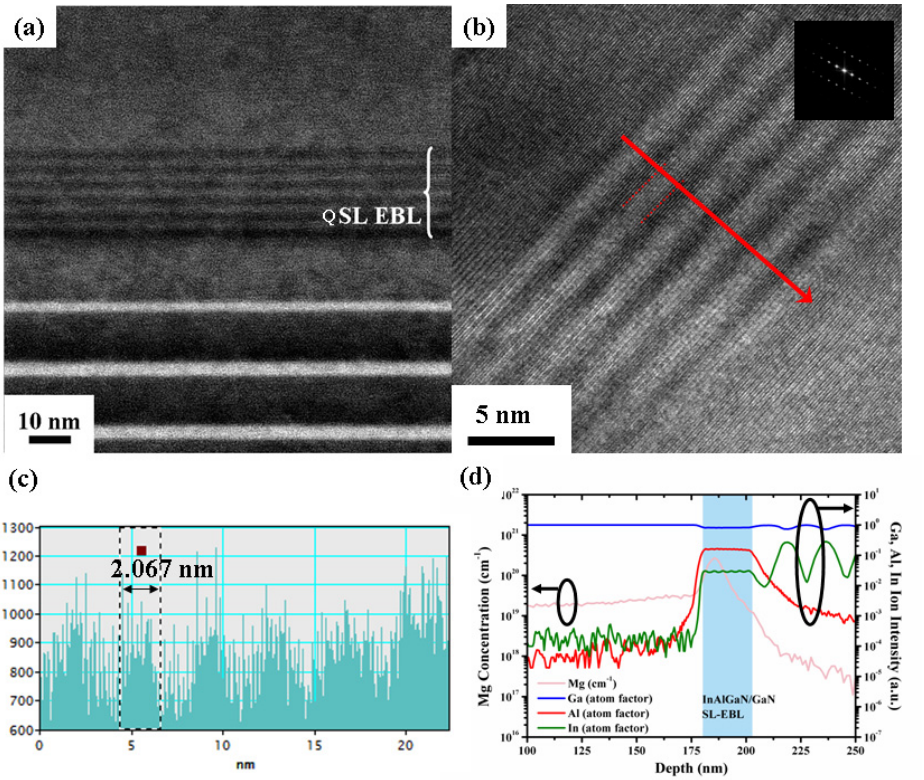

Fig. 2. (a) STEM-HAADF image and (b) high resolution bright field image of QSL-EBL. The fast Fourier transform (FFT) image is shown in the inset, presents the zone axis of g = [1 $\bar{1}$ 00]. (c) The intensity line profile of QSL-EBL, which was corresponded to the red line form Fig. 2(b). (d) The SIMS spectra of Ga, Al, In, and Mg atoms, which was performed form the QSL-EBL structure.

The optical and electrical properties of LEDs were investigated by APSYS simulation software, which was developed by *Crosslight Software Inc*. The simulated structures, such as layer thicknesses, doping concentrations, and aluminum composition are the same as the actual devices. Commonly accepted physical parameters were used to perform the simulations. The percentage of screening effect was 40%, the Shockley-Read-Hall recombination lifetime was 6 ns, the internal loss was 2000 m^{-1}, and the Auger recombination coefficient in quantum wells (QWs) was with the order of 2×10^{-31} cm^6/s, respectively. In our study, a band offset ratio of 67/33 for the all interface is assumed principally. The 170 meV of Mg activation energy for GaN which is assumed to increase by 3 meV per Al% for AlGaN. Other material parameters used in this simulation can be found in [29].

3. Results and discussion

Figure 3 shows the simulated electrostatic fields of bulk-EBL LED, bulk-QEBL LED, and QSL-EBL LED near the active regions at 100 A/cm^2, respectively. The positions of the six quantum wells and EBLs are marked with gray areas and salmon regions, respectively. It is worth noting that the electrostatic field at the last barrier is actually negative, which means that the negative field would favor holes into MQWs. Figure 3(a) shows the electrostatic fields at the last barrier of bulk-EBL LED, bulk-QEBL LED, and QSL-EBL LED are -2.3×10^5 and -2.9×10^5, and -3.7×10^5 V/m, respectively. The electrostatic field at the interface between the last barrier and EBL was precisely reduced due to the lower polarization effect regarding the degraded lattice mismatch between GaN and $In_{0.03}Al_{0.20}Ga_{0.77}N$ layer. As shown

#261098 Received 22 Mar 2016; revised 6 Apr 2016; accepted 9 Apr 2016; published 17 May 2016

in Fig. 3(b), there are stronger electrostatic fields in the last quantum well of bulk-EBL LED and bulk-QEBL LED, which lead to the band bending and poor overlap of wave functions thereby reducing the radiative recombination rate. Figure 3(c) shows the calculated energy band diagrams of three LEDs at 100 A/cm^2. As shown in Fig. 3(c), the overall energy band will be pulled away from the MQW active region to improve the effective barrier height for electrons due to the negative electrostatic field was reduced at the last barrier/EBL interface. Compared to bulk-EBL LED, the QSL-QEBL LED shows a higher electron barrier height but a lower barrier height for holes. The effective barrier height for electrons was increased from 231 meV to 306 meV, while the effective barrier height for holes was reduced from 244 meV to 210 meV. This result is attributed to polarization-matched QSL-EBL regarding the raised electrostatic field at the interface between the last barrier and EBL. This improvement suggests that the lower negative electrostatic field in InAlGaN of QSL-EBL than in bulk-QEBL and bulk-EBL. Therefore, the QSL-EBL not only suppressed the electron overflow but also improved the hole injection efficiency.

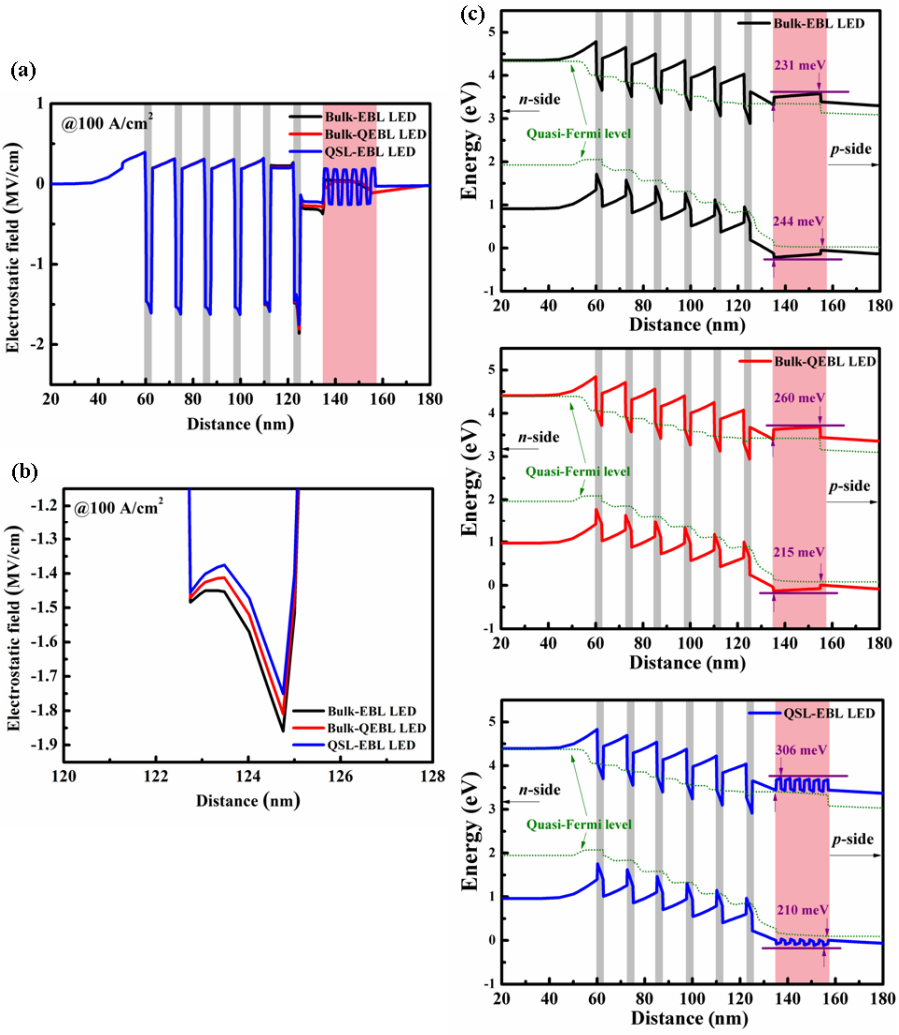

Fig. 3. (a) The calculated electrostatic fields of the LEDs with proposed EBL designs at 100 A/cm^2. (b) The zoom-in comparison of the electrostatic field at the last quantum well. (c) Energy band diagrams of the LEDs with proposed EBL designs at 100 A/cm^2. The effective barrier heights are marked in the figures.

#261098 Received 22 Mar 2016; revised 6 Apr 2016; accepted 9 Apr 2016; published 17 May 2016

The calculated distributions of electron and hole carriers within the active region at 100 A/cm^2 for LEDs are shown in Fig. 4. In Fig. 4(a), we can find out the more electrons are confined in the quantum wells and no severe electron accumulation at the interface between the last barrier and QSL-EBL. This result was caused by lower electrostatic field in the last barrier, as compared with the bulk-EBL LED and bulk-QEBL LED. In addition, we can observe that the more holes can be injected into active region, as shown in Fig. 4(b). As a result, the radiative recombination rate of QSL-EBL LED is higher than bulk-EBL LED and bulk-QEBL LED, as shown in Fig. 4(c). The fact means that we can obtain a uniform carriers distribution via QSL-EBL design, leading to preferable radiative recombination rate and EQE. Furthermore, we can also expect that the electron leakage can be eliminated, which was attributed to the improved barrier heights for electrons.

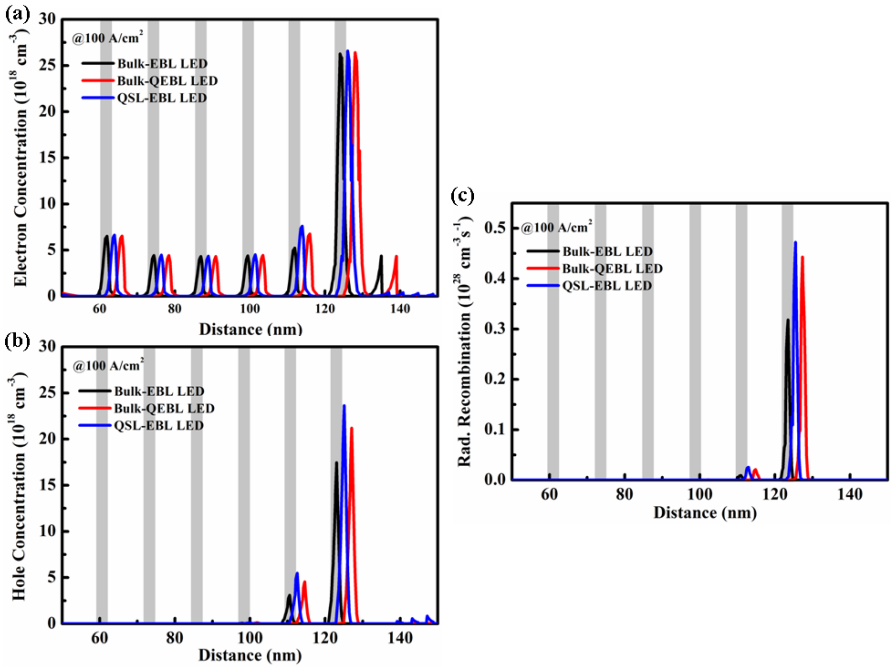

Fig. 4. (a) Electron concentration distributions, (b) hole concentration distributions, and (c) radiative recombination rates within the active regions of green LEDs with proposed EBL designs at 100 mA/cm^2.

The calculated electron reflectivity as a function of the incident electron energy for LEDs is shown in Fig. 5(a). The QSL-EBL can be able to produce higher refiective energy band than that of LEDs with bulk-EBL by means of the quantum interference. This may be resulted in the increasing of the effective barrier height for electrons and then prevent the electrons overflowing from the active region. However, deep dips can be found inside the reflectivity spectrum of the QSL-EBL LED at low energy range (100-150 meV). It means that the electron tunneling may be more easier in the QSL-EBL than in bulk EBLs. This may be attributed to the reduction of the total barrier thickness of QSL-EBL. Furthermore, Fig. 5(b) shows the electron current density profiles near the active regions for LEDs at 100 A/cm^2. The electron current density and the electron concentration were investigated by drift-diffusion model. As shown in Fig. 5(b), the electron leakage can be suppressed by introducing quaternary EBL, especially the lowest leakage was obtained by QSL-EBL. This result not only consists with the calculated electron reflectivity calculation but also completely compatible to higher effective barrier height. Although the bulk-QEBL shows polarization matched improvement than in bulk-EBL, but the electrostatic field was still higher than QSL-EBL in the last barrier, leading to a stronger electron leakage. Therefore, the superior band

#261098 Received 22 Mar 2016; revised 6 Apr 2016; accepted 9 Apr 2016; published 17 May 2016

alignment engineering results in lower electron leakage and uniform carriers distribution, hence the QSL-EBL is promising in higher EQE but with lower droop behavior.

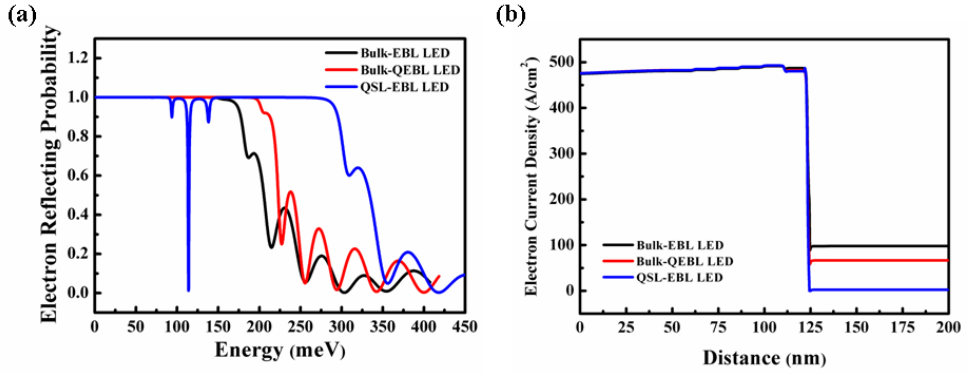

Fig. 5. (a) Electron reflecting probability and (b) electron current density for green LEDs with proposed EBL designs at 100 A/cm^2, respectively.

The experimental light output power (LOP) and EQE curves as a function of injected current density for bulk-EBL LED and QSL-EBL LED are shown in Fig. 6, respectively. The simulation results are well fitted to our experimental results. The LOP of QSL-EBL LED shows a 53% enhancement at 100 A/cm^2 as compared with bulk-EBL LED. We can see that the peak efficiency (η_{peak}) of QSL-EBL LED is increased at higher current density of 17 A/cm^2. The most important result is the reduction of efficiency droop, defined as ($\eta_{peak} - \eta_{100\ A/cm^2}$) / η_{peak}, which is reduced from 52% to 30% for QSL-EBL LED. The droop behavior consists to our simulations, which means that we can sum up the original reasons of droop improvement via QSL-EBL for green LED. This significant improvement of efficiency droop might be attributed to the enhancement of hole injection and electron confinement, implies that the polarization matched QSL-EBL is a good solution for high efficiency InGaN-based green LED.

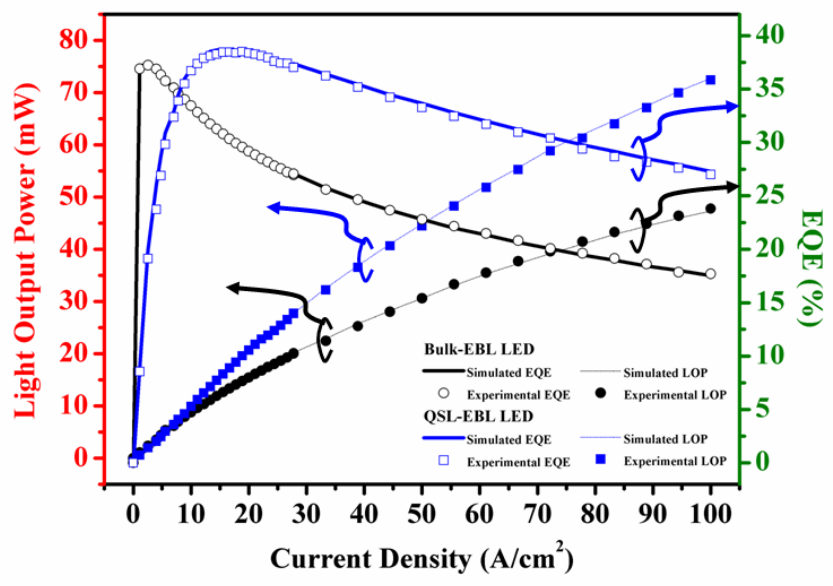

Fig. 6. Measured LOP and EQE curves as a function of the injection current density for LEDs. The experimental EQE and LOP data were plotted as symbols and well fitted to the simulations as lines.

#261098 Received 22 Mar 2016; revised 6 Apr 2016; accepted 9 Apr 2016; published 17 May 2016

5. Conclusion

In summary, the quaternary InAlGaN/GaN superlattice electron blocking layer (QSL-EBL) for the use of the InGaN-based green LEDs has been fabricated and analyzed through the digital growth method and band diagram simulations, respectively. The structural analysis by TEM and SIMS show that the digital growth method is a feasible to grow QSL-EBL structure. According to our investigations by simulation, the electrostatic field can be effectively reduced and further pulled up the energy band in the last GaN barrier. The effective barrier heights of the electrons and holes are also improved, leading to preferable radiative recombination rate and better LED efficiency performance at high current density. Compared to the conventional LED with bulk-EBL, the QSL-EBL LED exhibits a 53% enhancement of light output power. The efficiency droop can be reduced from 52% to 30%, suggesting that the LED with novel QSL-EBL structure is promising for future white lighting with superior color rendering.

Acknowledgment

This work was funded by the Ministry of Science and Technology in Taiwan under grant number, MOST 104-3113-E-009-002 -CC2.

#261098 Received 22 Mar 2016; revised 6 Apr 2016; accepted 9 Apr 2016; published 17 May 2016